Journal of Saudi Chemical Society (2017) **21**, 487–494

King Saud University

Journal of Saudi Chemical Society

www.ksu.edu.sa
www.sciencedirect.com

ORIGINAL ARTICLE

Activated carbon from orange peels as supercapacitor electrode and catalyst support for oxygen reduction reaction in proton exchange membrane fuel cell

M. Dhelipan [a], A. Arunchander [b], A.K. Sahu [b], D. Kalpana [b,*]

[a] *Ingsman Energy and Fuel Cell Research Organization Pvt. Ltd, Chennai, India*
[b] *CSIR – Central Electrochemical Research Institute – Madras Unit, CSIR Campus, Taramani, Chennai 600 113, India*

Received 26 August 2016; revised 16 December 2016; accepted 20 December 2016
Available online 28 December 2016

KEYWORDS

Orange peels;
Activated carbon;
Surface area;
Supercapacitors;
PEM fuel cell;
Catalyst support

Abstract Activated carbon is synthesized using orange peel as precursor through chemical activation using H_3PO_4 and its ability as electrocatalyst support for ORR reaction is examined. The prepared material was subjected to various structural, compositional, morphological and electrochemical studies. For ORR activity, the platinum loaded on activated carbon (Pt/OP-AC) was investigated by cyclic voltammograms (CVs) recorded in N_2 and O_2 saturated 0.1 M aqueous $HClO_4$. For supercapacitor performance, three electrode systems was tested in aqueous H_2SO_4 for feasibility determination and showed electrochemical double layer capacitance (EDLC) behaviour which is expected for activated carbon like materials. Electrochemical surface area (ECSA) of the activated carbon from orange peel is measured using CV. The physical properties of the prepared carbon are studied using SEM (scanning electron microscope), XRD (X-ray diffraction), Fourier transform infrared (FT-IR) spectroscopy and Raman spectroscopy. The AC derived from orange peels delivered a high specific capacitance of 275 F g^{-1} at 10 mV s^{-1} scan rate. Hence, this study suggested that orange peels may be considered not only as a potential alternative source for synthesizing carbon supported catalyst for fuel cell application but also highlight the production of low-cost carbon for further applications like supercapacitors.

1. Introduction

Polymer Electrolyte Membrane Fuel Cell (PEMFC) has viable potential as next generation power source, especially for portable applications due to its high power density and zero or low emission of pollutant [1–4]. However, commercialization of fuel cell is hindered by high cost and limited resource of platinum catalyst. Prodigious research efforts have been made

* Corresponding author. Fax: +91 044 22544526.
E-mail address: drkalpanaa@gmail.com (D. Kalpana).
Peer review under responsibility of King Saud University.

Production and hosting by Elsevier

http://dx.doi.org/10.1016/j.jscs.2016.12.003
1319-6103

to overcome the cost of fuel cell by using non-noble catalyst and ultra-low platinum catalyst with high surface area catalyst support. Carbon has more advantage than metal oxides as electrocatalyst support in terms of high specific surface area, high stability in acidic and basic media and easy recovery of metal catalyst by burning off the carbon support. The widely used material as electrocatalyst support is carbon black but it still suffers from setbacks like corrosion and deep micro porous, where the catalyst nanoparticles are trapped and failed to achieve three phase interface. However in the past decades, many efforts have been done for fabricating high surface area activated carbon (AC) from agricultural waste such as grass, nut shells etc. [5], which would drastically reduce the cost of production of activated carbon. Conversion of waste into AC reduces the cost of waste disposal and provides an economic alternative to the conventional method of fabricating AC [6]. Many literatures are available for synthesizing low cost AC from agriculture waste such as groundnut shell [7], coconut shell [8], palm oil shells [9], mango nuts [10], olive stone [11], waste cherry stones [12], Neem husk [13], Peanut hulls [14], paper mill sludge [15], banana fibres [16], sunflower seed oil [17] and sugarcane bagasse [18] etc. But very few literatures are available on using AC derived from orange peels as electrocatalyst support for fuel cell application.

Activated carbons are mostly used in commercial supercapacitors as electrode material because of their good electrochemical stability, high surface area, electrochemical properties etc. As the application of AC is increasing day by day, the large scale production of AC is hindered by increasing raw material cost and less availability of precursors. However fossil fuels do not meet this demand as they are not renewable in nature. Hence, utilization of bio-waste as precursor for production of AC can fulfil the demand because of their low-cost accessibility.

In this work, orange peels (Citrus Sinensis) are utilized as a precursor for production of activated carbon and the same will be used as a support material for platinum catalyst. The orange peels are chemical activated using H_3PO_4 acid. Fernandeza et al. synthesized activated carbon from orange peels using H_3PO_4 acid as a activator for removing basic dyes (methylene blue and rhodamine B) from single and binary dyes solutions in continuous and batch modes. This type of activated carbon from orange peels has high surface area of 1090 $m^2 g^{-1}$ [19] which is higher than commercially used Vulcan XC-72 (250 $m^2 g^{-1}$) [20]. Arie et al. used AC from orange peels as an electrode material for lithium ion capacitors [21]. The physical morphology of the prepared AC will be analyzed using SEM, XRD and Raman shift. Furthermore the electrocatalytic properties of the electrode coated with platinum reduced carbon support will be studied using CV and LSV. Fuel cell performance of the MEA fabricated using the prepared electrode for ORR will be studied using fuel cell workstation. This type of AC using orange peels as precursor for fuel cell catalyst support is first of kind ever reported.

2. Experimental

2.1. Preparation of orange peels derived activated carbon (OP-AC)

The orange peel was dried at 100 °C for 8 h. In a typical synthesis experiment, 60 g of orange peel was mixed with 15 g of phosphoric acid (H_3PO_4) in 100 mL of distilled water. The mixture was stirred at room temperature for 24 h and then dried in a furnace at 100 °C. Carbonization was performed in a tube furnace under argon gas flow and at a heating rate of 600 °C. The maximum temperature was held for 24 h. The carbonized samples were rinsed with distilled water followed by acetone, filtered and then dried at 100 °C for 24 h.

2.2. Preparation of Pt/OP-AC electrode for electrochemical studies

Pt was successfully deposited on OP-AC by chemical reduction method. Typically, 0.3 g OP-AC was dispersed in 50 mL DI water and sonicated for 30 min. Then, 200 mg H_2PtCl_4 was dissolved in 50 mL of DI water and added to the carbon dispersion. The mixture was stirred for 1 h and 3 M $NaBH_4$ in 0.3 M NaOH solution was added to it. Further the mixture was stirred for 1 h for the reduction of Pt^{2+} to Pt. The above mixture was filtered and washed thoroughly with copious amount of DI water. Then the product was dried at 80 °C overnight.

2.3. Physical characterization of OP-AC

Surface morphology of OP-AC is analysed using SEM image which is performed in Vega3Tescan. X-ray diffraction patterns were recorded between 10° and 90° on PW3040/60 X'pert PRO diffractometer with Copper radiation sources. Surface functionalities of the prepared OP-AC were identified using FT-IR (BrukerOptik GmbH), Raman spectroscopy was conducted to evaluate the graphitic character of the sample and the surface area of the sample is measured by BET method.

2.4. Electrochemical characterization of Pt/OP-AC

Electrochemical properties of the catalyst were measured by cyclic voltammetry (CV) and Linear Sweep Voltammetry (LSV) studies using BioLogic potentiostatat room temperature (25 °C). The glassy carbon (GC) disk electrode with the area of 0.071 cm^2 was considered as the working electrode. Prior to use, the GC was polished with 0.3 μ alumina powder till to get mirror finish. To prepare the working electrode, Pt/OP-AC slurry was made by ultrasonically dispersing 2.13 mg Pt/OP-AC in 0.9 mL DI water and 0.1 mL iso-propyl alcohol mixture with 5 wt% Nafion solution for 30 min. Then, 5 μL of the catalyst ink was dropped on to the top of the GC electrode and dried at room temperature to obtain Pt loading of 30 μg cm^{-2}. A Pt wire and a saturated calomel electrode (SCE) were used as counter and reference electrodes, respectively in a standard three-electrode electrochemical cell. All potentials are reported in terms of the reversible hydrogen electrode (RHE) scale for convenience. Hydrogen adsorption–desorption voltammograms were recorded in 0.1 M $HClO_4$ aq. solution at a scan rate of 50 mV s^{-1} purging with N_2 gas to remove dissolved O_2. The region for hydrogen adsorption between 0.05 V and 0.4 V vs. RHE on the backward potential scan was used to estimate the electrochemical surface area (ESA). Linear Sweep Voltammetry (LSV) for oxygen reduction reaction (ORR) measurements was performed in aqueous 0.1 M $HClO_4$ saturated with O_2 at a scan rate of 5 mV s^{-1}. For supercapacitor performance, the electrode was prepared as

reported in the previous studies [22]. The resistance of the sample is measured by using impedance spectroscopy.

Performance of the MEA was analysed by Biologic Fuel cell test station. Evaluation has been done at the fuel cell temperature of 60 °C. Pt/OP-AC was used as a cathode catalyst and commercial catalyst as anode. The membrane was sandwiched between the electrodes. The inlet gases were maintained at the pressure of 2 bar and flow rate of hydrogen

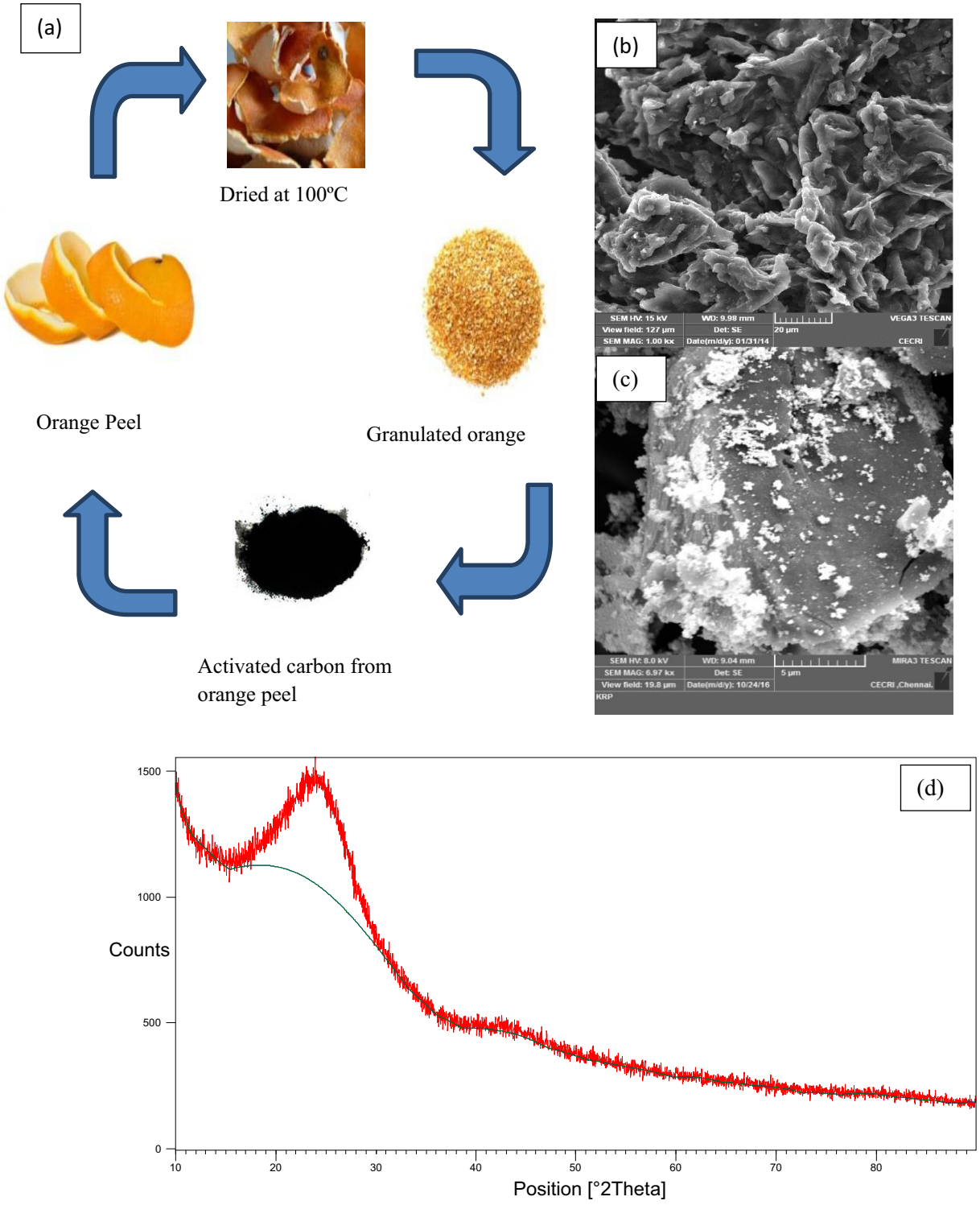

Fig. 1 (a) Fabrication process of OP-A.C (b) SEM micrograph of OP-AC. (c) Sem micrograph of Pt/OP-AC. (d) XRD pattern of OP-AC.

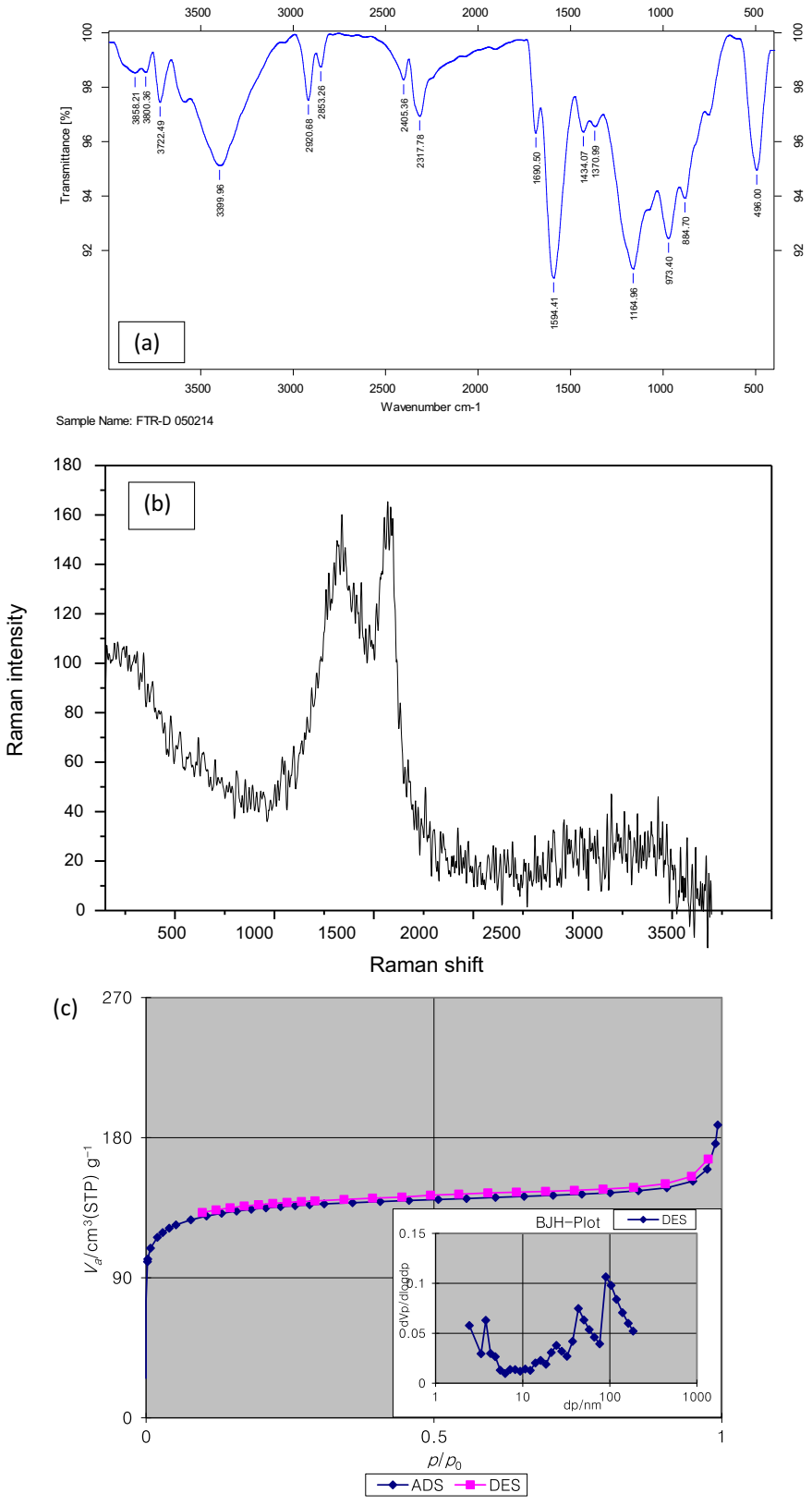

Fig. 2 (a) FTIR spectrum of OP-AC. (b) Raman spectra of OP-AC. (c) Adsorption/desorption isotherm of OP-AC.

and oxygen were 1000 mL min^{-1}. The MEA was activated for 5 h by supplying hydrogen and oxygen from the electrolyser, followed by hydrogen and oxygen from compressed cylinder for 5 h at cell temperature, 80 °C. The constant voltage of 0.4 V is maintained during activation with 100% RH for inlet gases.

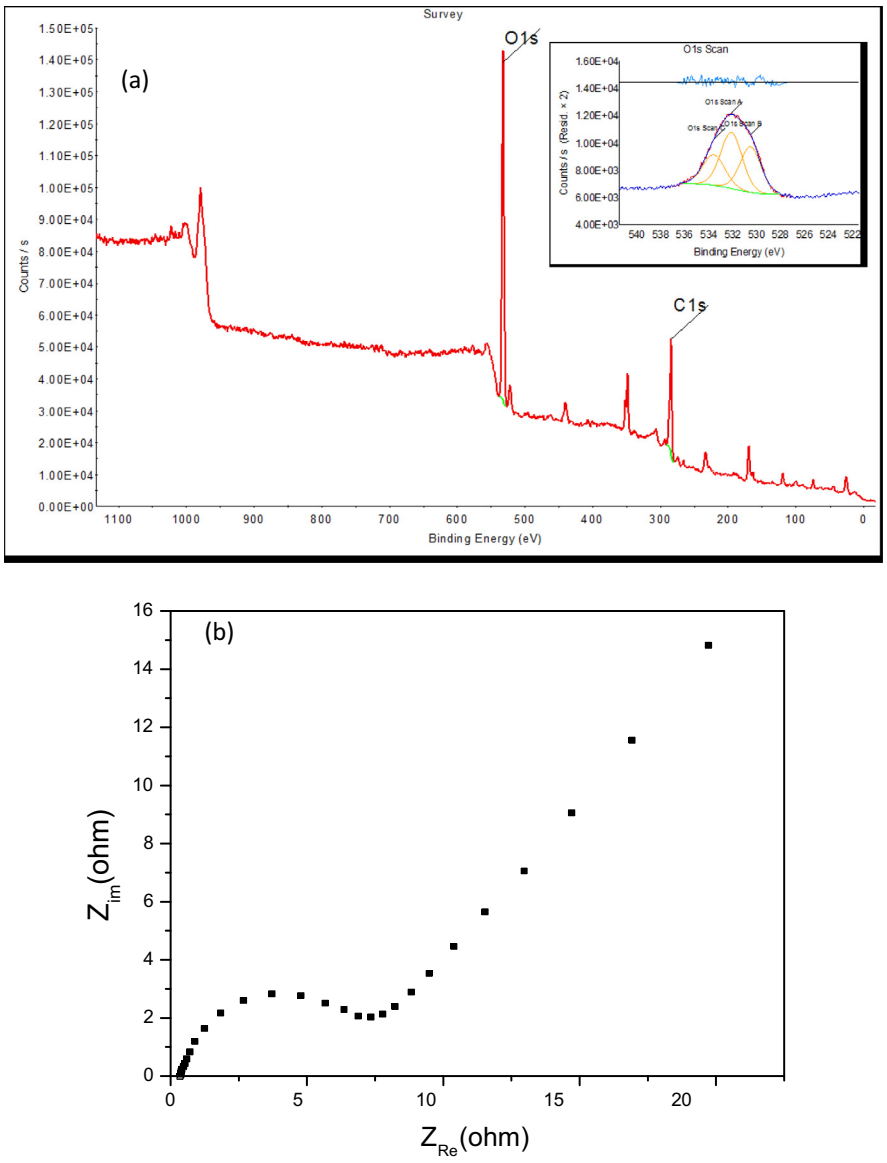

Fig. 3 (a) XPS analysis for OP-AC with O1s spectra of oxygen inside. (b) Nyquist plot of OP-AC.

3. Results and discussion

The preparation process is illustrated in the Fig. 1a. Scanning electron microscope was used to observe the surface morphology of the sample. The Fig. 1b shows the SEM images of the OP-AC which has smooth surface and irregular intercellular spacing and the change in the morphology can be observed in the SEM image (Fig. 1c) of Pt/OP-AC. The crystallinity of the prepared activated carbon from orange peel was characterized by using the X-ray diffraction method. The XRD patterns of activated carbon from orange peel prepared at 600 °C for 24 h is shown in Fig. 1d. The diffraction pattern of the as prepared OP-AC at $2\theta = 22.57°$ and 42° corresponds to the reflections of (0 0 2) and (1 0 0) planes, respectively. The broad XRD peak indicates that carbon is highly amorphous and similar trend was observed in the results of Xie et al. [23].

Fig. 2a shows the FTIR spectroscopy for OP-AC. It is very useful technique to identify functional groups, structure determination, identification of organic compound and study of chemical groups. The peak at 496.00 cm^{-1} is due to C—C stretching, the absorption peaks at 3399.95 cm^{-1} and 3722.49 cm^{-1} corresponds to the stretch vibration of —OH [23]. Peak at 1690.50–1594.41 cm^{-1} is corresponds to the stretching vibration absorption of C═O and, the peak at 1164.96 cm^{-1} is due to vibration absorption of C—O.

The intensity of Raman spectral lines are characterized by using the Raman spectroscopy which is shown in the Fig. 2b. The Raman spectra was carried out in the range of 500–3500 cm^{-1}. The Raman spectra of the sample composed of two peaks around 1598 cm^{-1} and 1350 cm^{-1} which are known as the G (graphitic or ordered) and D (disordered) band respectively. The defect in the spectra shows that the sample contained sp^2 carbon network which can exist in either C═C chains or aromatic ring structure. The Raman spectra for given sample shows broad peaks, which is the characteristics of the amorphous nature of carbon and the intensity ratio

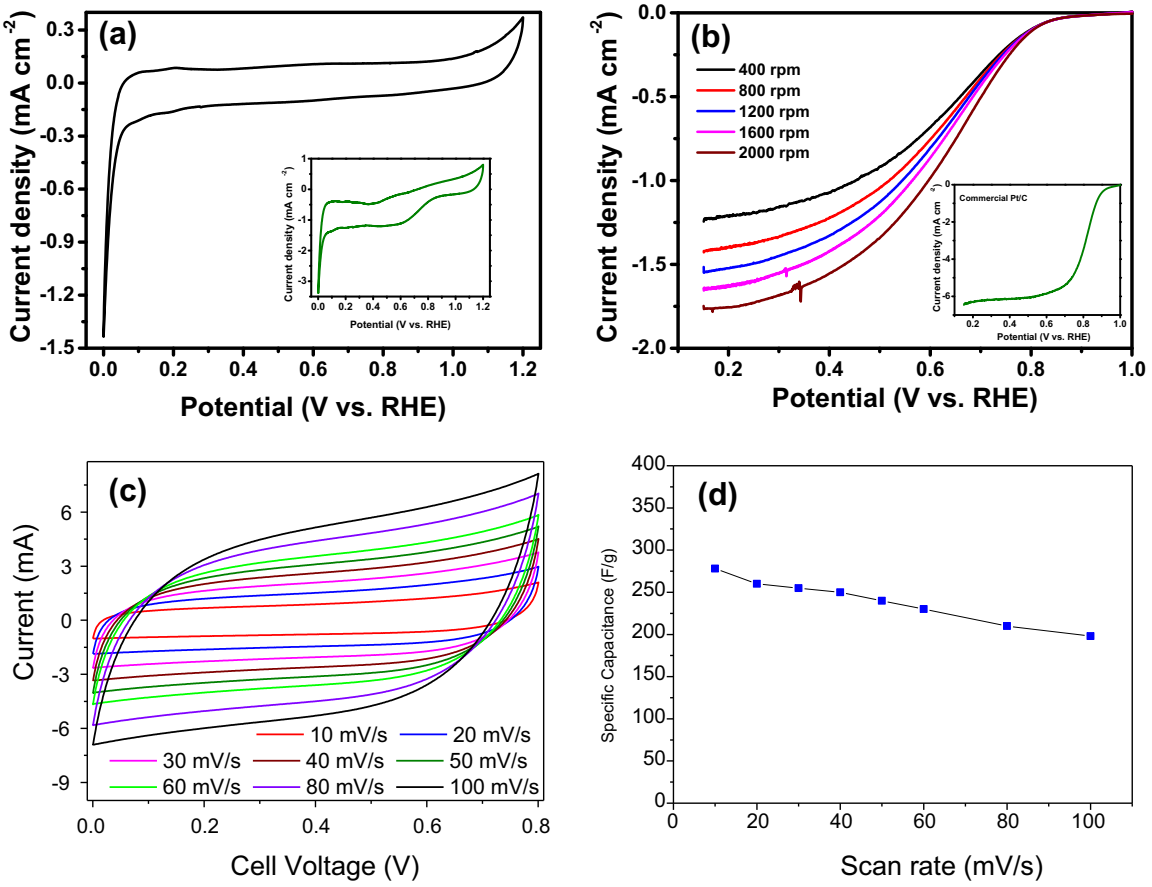

Fig. 4 (a) Cyclic voltammogram of Pt/OP-AC. (b) LSV of Pt/OP-AC with different rotation speed. (c) CV curves at different scan rates. (d) Specific capacitance as a function of the current density. (e) Specific capacitance with respect to scan rate.

(I/I) for the prepared carbon is 1.032 which shows the ordered nature of the carbon. The results are coherent with the activated carbon prepared by Kishore et al. [24].

The Brunauer–Emmett–Teller (BET) surface area of the sample is determined by nitrogen adsorption at 77 K. Nitrogen adsorption/desorption isotherms for orange peel activated carbon is illustrated in Fig. 2c. The volume of nitrogen adsorbed per sample mass unit are represented as a function of the relative pressure (p/p_0), where p is the equilibrium pressure and p_0, the saturation pressure of the adsorbate. The adsorption isotherm of OP-AC presented essentially a type II shape which confirms the presence of pores [25], according to the IUPAC classification and the presence of desorption hysteresis loop H4 type is observed which is associated with slit shaped pores [26]. The pore volume and diameter of the sample is 0.088859 $cm^3\ g^{-1}$ and 90.22 nm which can be seen in the Fig. 2c (inside).

The XPS of OP-AC indicates the presence of two distinct peaks at 534.5 and 285 eV which can be attributed to oxygen and carbon respectively. Fig. 3 shows the XPS analysis for OP-AC with O1s spectra of oxygen inside. The oxygen content in the sample was 50.8% which shows that abundant surface oxygen functional group (hydroxyl and carboxyl) are present in the sample. There are three curves for O1s scan with binding energies 530.5, 532.5, 533.8 eV attributed to C═O, C─O, O─C═O. Presence of oxygen or oxygen containing elements can increases the resistance by hindering the hydronium (H_3O^+) ion penetration into micropores layer due to steric hindrance which intense reduce the fuel cell performance [27].

The imaginary part of the impedance tends to zero at high frequency. The measured resistances consist of contact resistance between the active material and current collector which can be neglected, ionic resistance of the electrolyte and intrinsic resistance of the active material. The presence of loop at higher frequency is described as pseudo transfer resistance [28] which is related with the porous structure of the electrode. At a potential of 10 mV the Nyquist impedance spectra is recorded within the frequency range of 20 kHz–0.01 Hz as shown in Fig. 3b. The semicircle observed in the middle frequency range reveals the charge-transfer resistance (R_{ct}), of 3.34 Ω. Shift in the appearance of capacitive behaviour (sharp increase of imaginary part) towards high value of resistance is observed in the loop which reveals the capacitive nature of the activated carbon. At low frequency the imaginary part increases sharply which is also due to the capacitance behaviour of the electrode.

Furthermore, the cost of obtaining OP-AC and commercially available VulcanXC-72 and 10% Pt catalyst supported on Vulcan XC-72 both purchased from Cabot Corp. are compared and presented here. The cost of Vulcan XC-72 from Cabot Corp. is reported to be USD 50.00/50 g and that of 10% Pt on Vulcan XC-72 is USD 69.00/g (www.fuelcellstore.com). Even though OP-AC was obtained from zero-cost biomass, commercial success could be achieved only if

the pore volume, structure and electrode stability during ORR in fuel cell are optimized. The intention of this study on the cost comparison is to enhance the research activities related to carbon production from orange peel or other biomass sources. However results from our preliminary investigation suggest that OP-AC may replace the traditional carbon supports in the near future.

Fig. 4a shows cyclic voltammogram of Pt/OP-AC. Electrochemical surface area (ECSA) of Pt of the electrocatalysts was estimated from the equation given below:

$$ECSA = \frac{Q_H}{[Pt] \times 210}$$

where Q_H is the charge of hydrogen desorption on the Pt surface ($\mu C\ cm^{-2}$), [Pt] represents the Pt loading ($\mu g\ cm^{-2}$) and 210 ($\mu C\ cm^{-2}$) represents the charge required to oxidize a monolayer of H_2 on Pt surface. CV was acquired in O_2 and N_2-saturated 0.1 M aqueous $HClO_4$ and the potential was swept between 0.0 V and 1.2 V (vs. RHE) at the scan rate of 50 mV s^{-1} with metal loading of 30 $\mu g\ cm^{-2}$. No distinguish peak is observed for N_2 saturated solution, whereas visible peak (Fig. 4a inside) at 0.6 V is observed for O_2 saturated solution where no other significant oxygen-dependent reaction except the oxygen reduction reaction can occur. The geometric area of the GCE is 0.071 cm^{-2} and the calculated ECSA is 17.8 $m^2\ g^{-1}$. Due to the larger pore diameter, the platinum materials were entrapped and this might be the reason for low ECSA.

Fig. 4b shows the linear sweep voltammogram (LSV) of Pt/OP-AC. LSV was measured 0.2–1.0 V with a sweep rate of 5 mV s^{-1} in O_2 saturated 0.1 M aqueous $HClO_4$ solution.

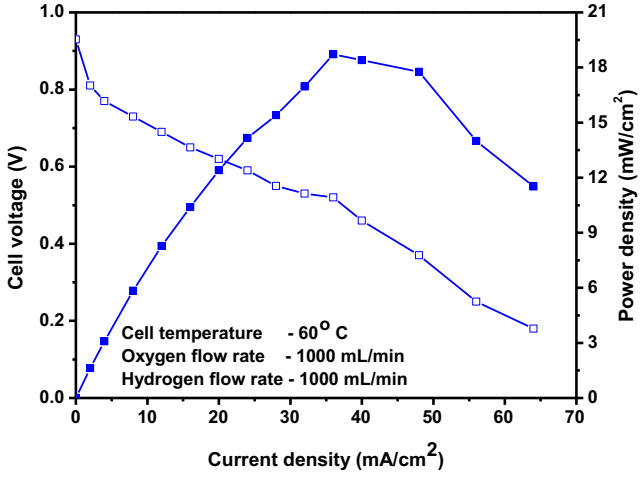

Fig. 5 Fuel cell performance of Pt/OP-AC as cathode catalyst.

The onset potential of catalytic current begins at 0.84 V and for Pt/OP-AC (Fig. 4b inside) at 1600 rpm speed, the onset potential is at 0.9 V. The limiting current density at 0.6 V is 1 mA cm^{-2} for Pt/OP-AC and for the Pt/C is 5.84 mA cm^{-2}.

The electrochemical properties of OP-AC electrodes were tested in 0.1 M H_2SO_4 using CV by three electrode system and the obtained results are shown in the Fig. 4c. The rectangular like behaviour of the CV curves show that the activated carbon from OP is capacitance and highly reversible [29]. The cyclic voltammogram reveals that the electrode is stable in acidic medium within the selected potential. In CV curves, the carbon displays a high current during the potential sweep is expected from the contribution of highly porous nature of the carbon. It gives maximum capacitance of 275 F g^{-1} at 10 mV s^{-1} scan rate.

As the scan rate increases the specific capacitance decreases gradually. Generally for AC's there is a linear relationship between surface area and capacitance. In the case of OP-AC, though the specific surface area is 640.3 $m^2\ g^{-1}$, the ability of charge accumulation at the electrode/electrolyte interface strongly depends as the ionic accessibility to the highly porous nature of the carbon. The specific capacitance (F g^{-1}) was measured from the rectangular CV curves for various scanning rate (10-100 mV s^{-1}) and current density (1–6 mA cm^{-2}). Typical behaviour of electrochemical supercapacitor is seen from the Fig. 4d and e where capacitance of the cell decreases linearly when the current density is increased [30,31]. Table 1 shows that the specific capacitance and surface area of OP-AC is higher than other organic derived activated carbon.

The MEA (membrane electrode assembly) prepared using Pt/OP-AC electrode shows peak power of 19 mW cm^{-2}. Fig. 5 shows the fuel cell performance of the MEA prepared using OP-AC. Presence of oxygen or oxygen containing elements can increases the resistance by hindering the hydronium (H_3O^+) ion penetration into micropores layer due to steric hindrance and the entrapment of platinum into the pores might be the reason for poor fuel cell performance and the MEA needs to be optimized by varying the Platinum loading on OP-AC which is out of scope of the present investigation.

4. Conclusion

Activated carbon from orange peel treated with orthophosphoric acid using pyrolysis method at 600 °C has been successfully prepared by the simple activation method. The X-ray diffraction confirmed that the carbon is highly amorphous and FTIR analysis confirmed the peaks at 496.00 cm^{-1}, 1164.96 cm^{-1} and 3399.96 cm^{-1} assigned to the stretching vibrations of C—C, C—O, O—H respectively. In Raman analysis the peak at nearly 1300 cm^{-1} due to disordered activated

Table 1 Specific capacitance and surface area for different organic derived activated carbon.

Material	Electrolyte	Surface area ($m^2\ g^{-1}$)	Capacitance (F g^{-1})	References
OP-AC	0.1 M H_2SO_4	508.68	275	(Our carbon)
Rubber wood sawdust-based AC	H_2SO_4	< 920	8–139	[32]
Banana AC	1 M Na_2SO_4	1097	74	[16]
Straw-based AC	Organic	2316	251	[33]
Sun flower seed shell-based AC	KOH	619–2585	220	[34]
Sucrose-based AC	Ionic liquid	817–1941	45–178	[35]

carbon, the peak at nearly 1500 cm^{-1} is due to ordered activated carbon. Cyclic voltammetric data of the OP-AC electrode indicates a specific capacitance of 275 F g^{-1} at a 10 mV s^{-1} scan rate. The Pt/OP-AC has electrochemical surface area of 17.8 m^2 g^{-1} and have performed well as catalyst support for Oxygen reduction reaction. It is suggested that the OP-AC may be a novel catalyst support material for fuel cells.

Acknowledgments

The authors thank Dr. V.V. Giridhar, scientist in charge, CECRI, Madras Unit, and Dr. Vijayamohanan K. Pillai, Director, CSIR-CECRI, for their constant encouragement and support.

Reference

[1] G. Avgouropoulos, G. Avgouropoulos, S. Schlicker, K.-P. Schelihaas, J. Papavasiliou, K.D. Papadimitriou, E. Theodorakopoulou, N. Goiurdoupi, A. Machocki, T. Ioannides, J.K. Kallitsis, G. Kolb, S. Neophytides, J. Power Sources 307 (2016) 875–882.
[2] A.J. Appley, J. Power Sources 69 (1996) 153.
[3] S.M. Javaid Zaidi, Takeshi Matsuura, Polymer Membranes for Fuel Cells, Springer, 2009.
[4] J. Larminie, A. Dicks, Fuel Cell Systems Explained, Wiley, Chichester, UK, 2003.
[5] Palanichamy Kalyani, Ariharaputhiran Anitha, Andre Darchen, Int. J. Hydrogen Energy 38 (2013) 10364–10372.
[6] Mohd Rafatullah, Othman Sulaiman, Rokiah Hashim, Anees Ahmad, J. Hazard. Mater. 177 (2010) 70–80.
[7] R. Malik, D.S. Ramteke, S.R. Wate, Indian J. Chem. Technol. 13 (2006) 319–328.
[8] M.K.B. Gratuito, T. Panyathanmaporn, R.-A. Chumnanklang, N. Sirinuntawittaya, A. Dutt, Bioresour. Technol. 99 (2008) 4887–4895.
[9] Kanokorn Hussaro, Am. J. Environ. Sci. 10 (2014) 336–346.
[10] A. Kwaghger, E. Adejoh, Int. J. Eng. Res. Dev. 1 (2012) 01–07.
[11] N. Spahisa, A. Addoun, H. Mahmoudi, N. Ghaffour, Desalination 222 (2008) 519–527.
[12] Michael G. Lussier, Jeffrey C. Shull, Dennis J. Miller, Carbon 32 (1994) 1493–1498.
[13] K.K. Alau, C.E. Gimba, B.Y. Nale, Arch. Appl. Sci. Res. 2 (2010) 451.
[14] Badie S. Girgis, Samya S Yunisi, Ashraf M. Soliman, Mater. Lett. 57 (2002) 164.
[15] Hwa-Young Kang, Sang-Sook Park, Yu-Sup Rim, Korean J. Chem. Eng. 23 (2006) 948–953.
[16] V. Subramanian, Cheng Luo, A.M. Stephan, K.S. Nahm, Sabu Thomas, Bingqing Wei, J. Phys. Chem. C 111 (2007) 7527–7531.
[17] K.-Y. Foo, B.H. Hameed, Biosour. Technol. 102 (2011) 9794.
[18] Suely Patrícia C. Gonçalves, Mathias Strauss, Fabrício S. Delite, Zaira Clemente, Vera L. Castro, Diego Stéfani T. Martinez, Sci. Total Environ. 565 (2016) 833–840.
[19] Maria Emilia Fernandez, Gisel Vanesa Nunell, Pablo Ricardo Bonelli, Ana Lea Cukierman, Ind. Crops Prod. 62 (2014) 437–445.
[20] Panagiotis Trogadas, Thomas F. Fuller, Peter Strasser, Carbon 75 (2014) 5–42.
[21] Arenst Andreas Arie, Hans Kristianto, Joong Kee Lee, ECS Trans. 53 (2013) 9–13.
[22] D. Kalpana, S.H. Cho, S.B. Lee, Y.S. Lee, Rohit Misra, N.G. Renganathan, J. Power Sources 190 (2009) 587–591.
[23] Zhigang Xie, Wei Guan, Fangying Ji, Zhongrong Song, Yanling Zhao, J. Chem. 2014 (2014) 9.
[24] Brij Kishorei, D. Shanmughasundaram, Tirupathi Rao Penki, N. Munichandraia, J. Appl. Electrochem. 44 (2014) 903.
[25] C. Sangwichien, G.L. Aranovich, M.D. Donohue, Colloids Surf. A Physicochem. Eng. Aspects 206 (2002) 313–320.
[26] Zhonghua Hu, M.P. Srinivasan, Ni. Yaming, Carbon 39 (2001) 877–886.
[27] Gang-Wei Sun, Wang Can, Liang Zhan, Wen-ming Qiao, Xiao-yi Liang, Li-cheng Ling, J. Mater. Sci. Eng. 2 (2008) 41.
[28] X. Andrieu, G. Crepy, L. Josset, in: Proceeding of the 3rd International Seminar on Double Layer Capacitors and Similar energy Storage Devices, Florida Educational Seminar, 1993.
[29] Santhakumar, Kannappan, Karthikeyan, Kaliyappan, Rajesh Kumar, Manian, Amaresh Samuthira, Pandian, Hao, Yang, Yun Sung, Lee, Jae-Hyung, Jang, Wu, Lu, arXiv:1311.1548, 2013.
[30] Zhangpeng Li, Jinqing Wang, Xiaohong Liu, Sheng Liu, Junfei Ou, Shengrong Yang, J. Mater. Chem. 21 (2011) 3397.
[31] Kaliyappan Karthikeyan, Dharmalingam Kalpana, Samuthirapandian Amaresh, Yun Sung Lee, RSC Adv. 2 (2012) 12322–12328.
[32] E. Taer, M. Deraman, I.A. Talib, A. Awitdrus, S.A. Hashmi, A. A. Umar, Int. J. Electrochem. Sci. 6 (2011) 3301.
[33] X. Li, C. Han, X. Chen, C. Shi, Microporous Mesoporous Mater. 131 (2010) 303.
[34] X. Li, W. Xing, S. Zhuo, J. Zhou, F. Li, S.-Z. Qiao, G.-Q. Lu, Bioresour. Technol. 102 (2011) 1118.
[35] L. Wei, G. Yushin, J. Power Sources 196 (2011) 4072.